

# Exploring AI-based System Design for Pixel-level Protected Health Information Detection in Medical Images

Tuan Truong<sup>1,\*</sup>, Ivo M. Baltruschat<sup>1</sup>, Mark Klemens<sup>1</sup>, Grit Werner<sup>1</sup>, and Matthias Lenga<sup>1</sup>

<sup>1</sup>Bayer AG, Berlin, Germany

\*tuan.truong@bayer.com

## ABSTRACT

De-identification of medical images is a critical step to ensure privacy during data sharing in research and clinical settings. The initial step in this process involves detecting Protected Health Information (PHI), which can be found in image metadata or imprinted within image pixels. Despite the importance of such systems, there has been limited evaluation of existing AI-based solutions, creating barriers to the development of reliable and robust tools. In this study, we present an AI-based pipeline for PHI detection, comprising three key components: text detection, text extraction, and analysis of PHI content in medical images. By experimenting with exchanging roles of vision and language models within the pipeline, we evaluate the performance and recommend the best setup for the PHI detection task.

## Introduction

Protected Health Information (PHI) is health-related data that can identify an individual, often found in medical records, images, or any documents and data elements generated during participation in healthcare services. Before sharing data, e.g., for research purposes, it is crucial to de-identify or pseudonymize it to minimize the risk of re-identification. This de-identification step is mandatory for any study to comply with the Health Insurance Portability and Accountability Act (HIPAA) and the General Data Protection Regulation (GDPR), and it is the responsibility of the data provider. De-identification is a complex process that involves many data types and formats, typically including a detection step followed by the redaction or pseudonymization of the identified PHI. Medical images are a rich source of PHI, which can be embedded as metadata (e.g., in DICOM headers) or burnt-in text within pixel data. The automatic detection of pixel-level PHI is challenging due to the diversity in text locations, font sizes, colors, and contexts. As the amount and types of medical data continue to increase, so does the risk of incomplete redaction of PHI. This could potentially lead to data breaches, significantly impacting both the victims and the healthcare sector and resulting in high costs for the responsible health authority<sup>1</sup>.

Several automatic tools aim to remove all burnt-in text, regardless of the content<sup>2</sup>. While this approach ensures no PHI texts exist, it also discards valuable information such as measurements or markers. Additionally, some tools could erroneously detect text imprints within the anatomical structures of the image. After the imprints are localized in the image, filtering the content requires a complex and deeper context analysis. For instance, not all patient identifiers are considered PHI. Patient identifiers belonging to the hospital system pose a high risk of identification and should be redacted, whereas patient identifiers used in clinical trials are valid for study analysis and should be retained in the image. Advanced automatic solutions for PHI detection are essential for managing the increasing amount of medical data, especially for retrospectively collected large datasets. Such solutions are expected to handle edge cases, which can involve various signaling words and phrases. Moreover, research sites can have flexibility in determining whether to include or exclude certain entities as PHI depending on the setting of their studies or clinical trials. For example, although all dates are considered PHI according to the HIPAA guidelines, the date of visit is necessary for clinical trials. To accommodate such flexibility depending on studies, the PHI detection tool must incorporate mechanisms to easily specify and adjust rules for detecting PHI.

Our study focuses on AI-based approaches for automatically detecting PHI as burnt-in pixels. Currently, there are a few solutions that utilize vision and language models from MD.ai<sup>3</sup>, Google<sup>4</sup>, and John Snow Labs<sup>5</sup>. These tools integrate both the vision and language components: the vision component detects and converts burnt-in texts into machine-encoded texts, while the language component identifies any PHI content in the extracted texts<sup>6</sup>. AI models used in optical character recognition (OCR) and name-entity recognition (NER) tasks are often employed to handle text recognition and classify the PHI content. Recently, large language models (LLMs) have become the preferred candidates for the language component due to their flexibility to configure and ability to understand complex language context in NER tasks, which has proven helpful in

detecting PHI in biomedical text<sup>6</sup>. Despite some general remarks concerning the deployment of these tools<sup>7,8</sup>, particularly on the non-deterministic behavior and cost of LLMs, there is a lack of comprehensive studies dissecting the setup of vision and language models within a PHI detection pipeline. In addition, as multimodal LLMs with visual capabilities are being released today<sup>9</sup>, the question remains whether they can be used to recognize PHI through end-to-end processing of images.

To address the above concerns, we make the following contributions in our study:

- We propose a PHI detection system comprising three modules: text localization, extraction, and analysis using state-of-the-art vision and language models (Figure 4).
- We simulate PHI imprints on public medical datasets across four modalities to facilitate further development and benchmarking within the research community. The imprints come from 16 categories, eight of which are considered PHI.
- We combine three models - YOLOv11, EasyOCR, and GPT-4o, into four different setups of a PHI detection pipeline and compare their performance (Figure 1). In each setup, a model can assume one or multiple roles. For example, EasyOCR can perform not only text extraction but also text localization, and GPT-4o can perform end-to-end PHI detection instead of only analyzing the semantic content of extracted texts.

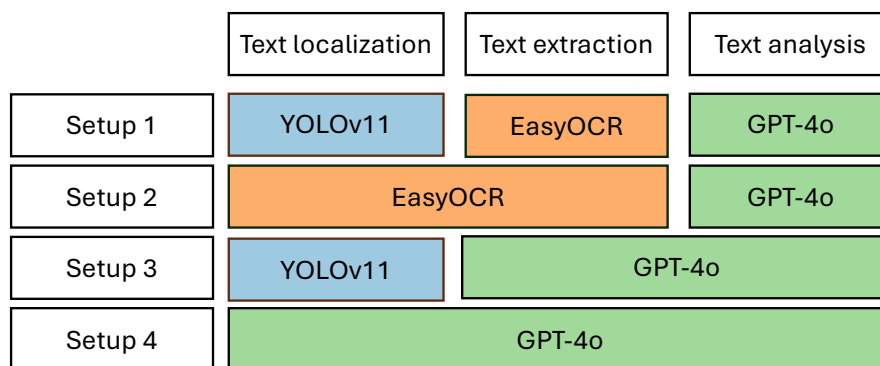


**Figure 1.** Four different setups in PHI detection pipeline.

## Dataset

### PHI Definition

For our experiments, we define a list of PHI and non-PHI items based on the HIPAA guidelines as detailed in Table 1. The eight PHI categories include date, general identifier, patient name, address, age, gender, phone number, and email. While the HIPAA guidelines recommend that only ages over 89 are considered PHI, we classify any age as PHI. This is to avoid re-identification, as age groups can exhibit skewed distribution depending on the study, making participants identifiable through age data. Additionally, we group all identification numbers into a group of identifiers, including patient ID, insurance number, social security number, and any number or series that can be used to identify an individual. The eight non-PHI categories include height, weight, examination type, hospital, marker, scanner, diagnosis, and imaging personnel.

### Datasets and Data Preprocessing

We select four well-known public datasets from the medical domain. Each of them was preprocessed before we added simulated imprints. In the following, we briefly describe each dataset and the applied preprocessing.

**Total Segmentator v2**<sup>10</sup> The dataset was originally published and used in a segmentation model for major anatomic structures in CT images. We use the second version, which includes 1,228 CT examinations across 21 scanners. Each volume is resampled to isotropic spacing of 0.45 mm across all three planes. Afterwards, four 2D axial slices are uniformly sampled per volume, which makes a total of 4,896 2D images. The images are min-max normalized to 8-bit format with the minimum value being random between the 0-th and 10-th percentile of the image intensities.

Category	Description	Is PHI	Example
Date	All elements of dates related to an individual, including birth date, admission date, discharge date, etc	PHI	DOB 01-01-2023
Identifier	All identifiers related to an individual such as patient ID, insurance number, medical record number, etc	PHI	Patient ID: 0000.0001
Patient name	Full name or initials of patient names	PHI	Pat. Name: John Doe
Address	Partial or full address of the patient that contains any of the following: street address, city, state, postal code, and country	PHI	123 Main St, Springfield, IL 62701, USA
Age	The patient's age at the time of the scan.	PHI	Age: 60
Gender	The gender of an individual, e.g., male, female, or diverse, or the abbreviations such as m/f/d	PHI	[M]
Phone number	Personal telephone number	PHI	Contact 794-512-9544
Email	Personal email address	PHI	Email: jane.smith@email.com
Height	Height measurement of the patient	Non-PHI	Height: 165 cm
Weight	Weight measurement of the patient	Non-PHI	Weight 103 kg
Examination type	The type of scan performed	Non-PHI	Exam: CT Cholangiography
Hospital	General information about the hospital or imaging facility	Non-PHI	Mayo Clinic Eau Claire
Marker	Text indicating anatomical markers or points of interest	Non-PHI	R POST L
Scanner	General information about the scanner type and scanner settings	Non-PHI	Philips Ingenia 3.0T
Diagnosis	General diagnosis, comments or indications made by doctors	Non-PHI	Diagnosis: Fibrosis
Imaging personnel	Information about the medical staff involved in the scan, such as names of the radiologist, technician, operator, or referring physician who orders, acquires, performs, or interprets the scan	Non-PHI	Indicated by John Moore

**Table 1.** Imprint categories and examples. There are 16 categories, eight of which are classified as PHI.

**BS-80K**<sup>11</sup> The dataset includes 82,544 radionuclide bone scan images of 13 body regions designed for classification and object detection tasks. Experts de-identified and annotated the images for classification and object detection tasks. For our experiments, we select subsets of whole-body images in anterior and posterior views. Due to the small size of whole-body images, we create image collages of three to five randomly repeated images. This approach mimics a bone scan viewer, where multiple views of a subject are displayed side by side for comparison. To enhance the diversity of bone scan variants, backgrounds are randomly flipped. The processed images are then saved in 8-bit format.

**ChestX-ray8**<sup>12</sup> The dataset contains 108,948 frontal X-ray images with nine disease labels parsed from radiological reports. Many images contain physical markers indicating left and right direction. To avoid confusion with added text imprints, we use an object detection model to identify these markers and apply center cropping to remove them. After cropping, the images are saved in 8-bit format.

**BRATS**<sup>13</sup> The dataset is part of the Medical Segmentation Decathlon and includes 750 brain MRI images from four sequences: native T1, post-contrast T1, T2-weighted, and T2-FLAIR. All images are resampled to isotropic spacing of 1 mm. For each subject, a random sequence is selected, and four 2D axial slices are uniformly sampled. The images are then min-max normalized to 8-bit format, following a similar approach to the Total Segmentator v2 dataset.

## Imprint Simulation

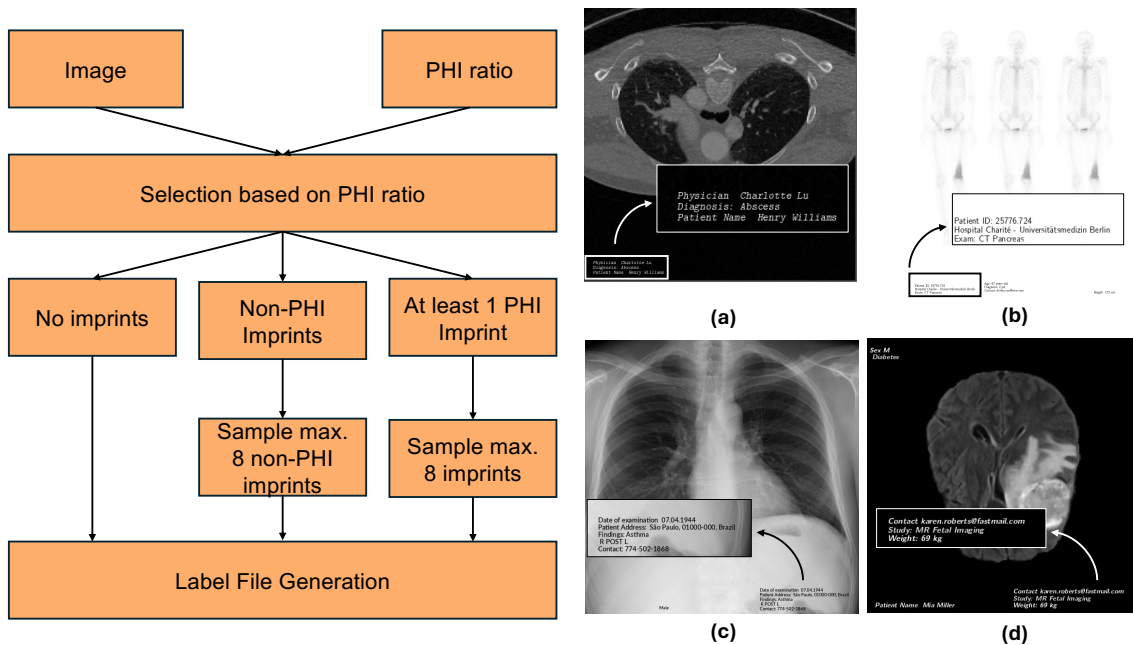


**Figure 2.** Imprint simulation pipeline and examples. (Left) Given the input PHI ratio for each dataset, each image can have no imprints, non-PHI imprints, or at least one imprint that contains PHI. The maximum of imprints per image is eight. (Right) Examples of images with imprints across four modalities: (a) Whole body CT (b) Whole body bone scan (c) Chest X-ray (d) Brain MRI.

The imprint simulation process is illustrated in Figure 2 (left). Based on the input ratio of PHI imprints for the simulated dataset, we determine for each image whether (1) no imprints are added, (2) only non-PHI imprints are added, or (3) at least one imprint includes PHI. Each image can contain a maximum of eight imprints. For each imprint category, as listed in Table 1, we generate imprints in the format <accompanying text> <separator> <main text>. The accompanying texts consist of signal words that indicate the category of the main text. The separator can be a comma , or a space. For example, in the text Patient Name: John Doe, Patient Name serves as the accompanying text, : is the separator, and John Doe is the main text. In some cases, we randomly omit the accompanying text, such as with identifiers where imprints may consist solely of a sequence of numbers. This omission tests the language model’s ability to infer the underlying imprint category robustly. After adding the imprints, a corresponding label file is generated. This label file contains the coordinates of each imprint in the image, along with its associated PHI class and sub-class. These labels are used for subsequent evaluation. The final dataset used to evaluate the PHI pipeline consists of 1,000 images distributed equally across four modalities. Of these,

850 images (85%) contain at least one PHI imprint. The distribution of the 16 imprint categories and the number of imprints per image are depicted in Figure 3.

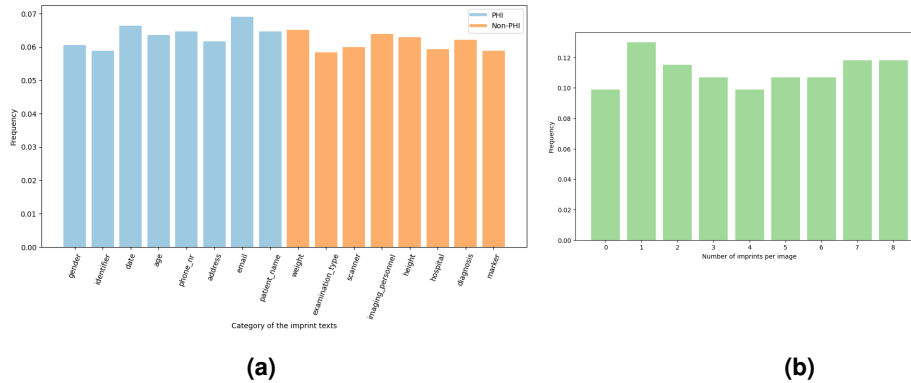


**Figure 3.** (a) Distribution of the imprint classes as generated in the simulated test dataset. In total, the test dataset contains 1,000 images. (b) The number of imprints per image.

## Methods

### PHI Detection Pipeline

Commonly, a PHI detection pipeline consists of three major modules: text localization, text extraction, and text analysis (see Figure 4). The text localization module can be an object detection model that identifies pixels containing texts in the input image and returns bounding box coordinates. Once the text coordinates are determined, the text extraction module converts the texts within these coordinates into machine-encoded texts, often using OCR algorithms. The machine-encoded text is then analyzed semantically by a language model, which classifies whether it contains any PHI. In the last step, the pipeline flags the image as containing PHI, prompting further review and potential redaction.

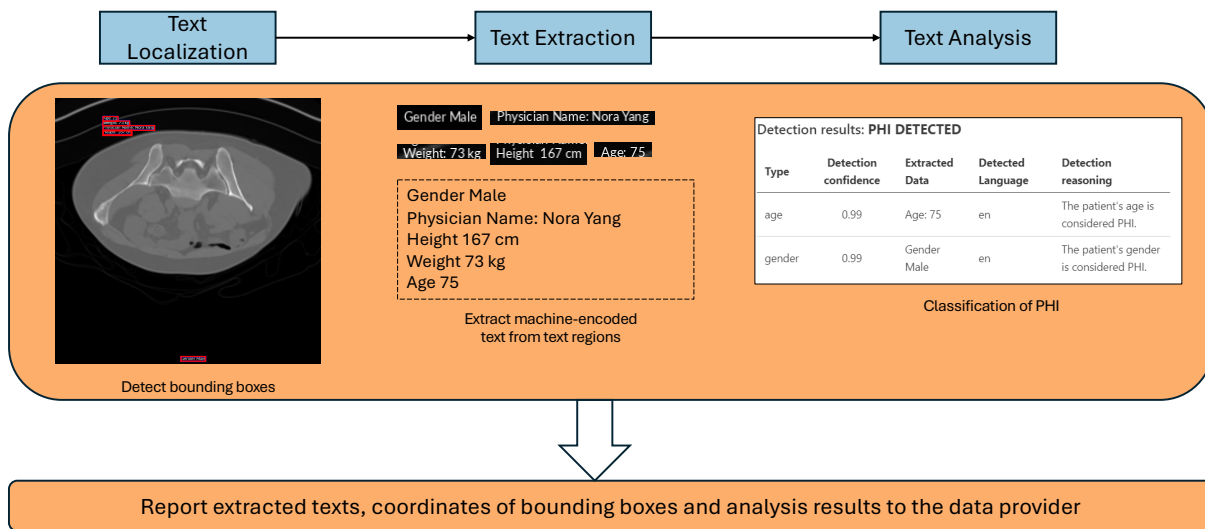


**Figure 4.** Pixel-level PHI detection pipeline. The pipeline consists of three components: text localization, text extraction, and text analysis. First, the bounding box coordinates of imprints are detected. Then, the text extraction module transforms the pixel-level imprints into machine-encoded texts. In the last step, the text analysis module identifies the PHI content.

**Text localization** YOLOv11<sup>14</sup> is the latest version in the series of YOLO models<sup>15</sup>, offering superior performance in real-time object detection tasks. Unlike multi-stage detection models with a longer inference time, YOLO models are single-staged, meaning each image needs only a single pass to generate the predictions. The YOLOv11 architecture consists of three primary

components: a backbone, a neck, and prediction heads. The backbone extracts image features, which are then processed and aggregated across multiple scales in the neck. The final predictions are produced by classification and detection heads. The main improvement in YOLOv11 is an optimized backbone and neck, which enhance the extracted features and enable more precise object detection. For our study, we use the small variant of YOLOv11 pre-trained on the COCO dataset and fine-tune it on our customized dataset that consists of CT, X-ray, and bone scan images with simulated text imprints. The model is trained to predict bounding boxes around a single line of text in the image, as illustrated in Figure 4. To make the model more robust, we simulate text imprints with diverse fonts, sizes, and locations, as shown in Figure 5 (left). In addition, we mix real medical images with synthetic images of diverse background colors and shapes to help the model be robust to any modality. We use the ultralytics package<sup>14</sup> to train the model with a fixed image size of 640x640 for 100 epochs. The other training arguments are kept as default in the package. Apart from regular geometric augmentation techniques, the images undergo mosaic augmentation, where a new image is created based on patches of original images, as shown in Figure 5 (top right). The mosaic augmentation helps the model to generalize better to diverse backgrounds and object locations.

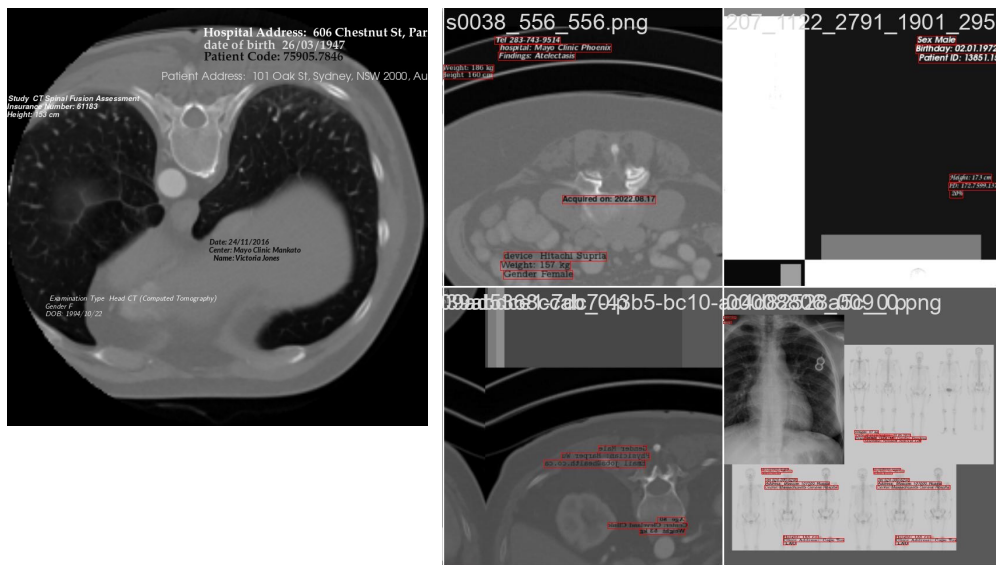


**Figure 5.** Examples of data used for training the localization model YOLOv11. **(Left)** Training image with multiple simulated text imprints in random locations **(Right)** Augmentation of training images. One of the augmentation schemes we use is mosaic augmentation, where the new image is created by blending multiple patches of original images.

**Text extraction** EasyOCR<sup>16</sup> is an open-source OCR package supporting over 80 languages. It comprises two primary modules: recognition and detection. The detection module, analogous to our localization module, identifies text regions in an image using the Character Region Awareness For Text detection (CRAFT) model<sup>17</sup>. The recognition module<sup>18</sup> extracts text by leveraging the Scene Text Recognition module, a multi-stage model that transforms input images, extracts features, aggregates contextual information, and finally outputs the characters. In this study, we use EasyOCR as an out-of-the-box tool without re-training or fine-tuning its components. We keep the values of all parameters as default except for the low-bound text threshold. We reduced this threshold to 0.2 to include more space around detected texts by the CRAFT model, which we found helpful in avoiding missing texts as single letters like markers (e.g., L or R) or abbreviations of gender (e.g., M or F or D). The input to EasyOCR can be either a full image or a cropped image of the text region detected by the localization model, which we perform the experiments (see [Experiment](#)) to compare these setups.

**Text analysis** GPT-4o<sup>9</sup> is OpenAI’s flagship language model in the Generative Pre-trained Transformer (GPT) family. These models are pre-trained on extensive unlabeled text datasets to generate human-like responses. GPT models have demonstrated their versatility in information extraction and NER tasks, particularly in biomedical text analysis. Leveraging the superior performance of GPT in information extraction, we use GPT-4o to analyze the context of extracted texts from images and determine whether they contain PHI. The extracted texts from the text extraction module are provided to GPT-4o as a list. The system prompt consists of the definition of PHI and non-PHI texts and instructions to evaluate the aggregated context of the input text rather than analyzing each line in isolation. To ensure consistent outputs, we constrain GPT-4o to produce a dictionary of mandatory fields through OpenAI’s pydantic tool, as outlined in Table 2. If the PHI is detected, the `type` field specifies

one of the eight PHI classes or `other` if the PHI category is not included in the provided list. If no PHI is detected, the text analyzer assigns `non-phi` to the `type` field. Additional fields include `raw_text`, `reason`, and `language`, which store the raw extracted text, the justification for classifying the text as PHI or non-PHI, and the detected language of the original text, respectively. The temperature parameter is set to 0 to yield more deterministic responses.

Tag	Data type	Description
<code>type</code>	<code>str</code>	One of [date, identifier, name, address, age, gender, phone_nr, email, other, non-phi]
<code>raw_text</code>	<code>str</code>	Original text extracted from the image
<code>reason</code>	<code>str</code>	Reason why the extracted text is considered PHI or not
<code>language</code>	<code>str</code>	Detected language

**Table 2.** Structure output of the text analyzer GPT-4o.

## Experiment

In this study, we assess various setups of a PHI detection pipeline by interchanging the roles of the presented models. Specifically, we study the four setups illustrated in Figure 1. The first setup employs three distinct models, each dedicated to one of the modules described in the [PHI Detection Pipeline](#) section. This serves as a baseline setup, where each model performs the task it is specifically designed for. In the second setup, we assess the robustness of EasyOCR’s built-in object detection capabilities by using it for both text localization and extraction tasks. EasyOCR handles the detection of text regions and subsequently extracts the corresponding text. The third setup evaluates the language-vision capability of GPT-4o by assigning the text extraction step to it. In this configuration, GPT-4o receives cropped text regions, localized by the YOLOv11 model, performs OCR, analyzes, and classifies PHI content. The final setup explores GPT-4o as an end-to-end solution. GPT-4o takes full responsibility for all three pipeline steps: localizing text in the image, extracting the text, and analyzing it for PHI content. This setup, in particular, highlights a new use case where a single language model integrates vision and language tasks, demonstrating the potential for end-to-end applications.

For each of the introduced setups, we evaluate the final output of the PHI pipeline in two stages. In the first stage, the pipeline is treated as a binary classifier for detecting PHI. The objective is to predict whether or not the image contains any PHI. In the second stage, only images identified as containing PHI are considered. The goal here is to evaluate whether the PHI categories are correctly classified. This stage functions as a multi-label classification task across eight PHI classes. For both stages, we compute the following performance metrics: accuracy, precision, recall, and F1 score.

## Results

	Precision		Recall		F1		Acc	
	Min	Max	Min	Max	Min	Max	Min	Max
Global PHI	0.9879	1.0000	0.9364	0.9976	0.9654	0.9988	0.9428	0.9990
Date	0.9394	1.0000	0.8759	1.0000	0.9339	1.0000	0.9669	1.0000
Patient Name	0.7411	0.9923	0.8591	0.9962	0.7958	0.9942	0.8933	0.9970
Address	0.8760	1.0000	0.9593	1.0000	0.9158	0.9980	0.9571	0.9990
Gender	0.9167	1.0000	0.6885	0.9549	0.8127	0.9749	0.9219	0.9879
Email	0.9955	1.0000	0.8453	0.9964	0.9162	0.9982	0.9568	0.9990
Phone Nr	0.9757	1.0000	0.8301	0.9961	0.9053	0.9981	0.9548	0.9990
Age	0.9267	1.0000	0.6523	0.9961	0.7877	0.9980	0.9096	0.9990
Identifier	0.8114	1.0000	0.8861	0.9747	0.8660	0.9871	0.9347	0.9940

**Table 3.** Minimum and maximum scores of precision, recall, F1, and accuracy for each PHI category. The color-coded cells correspond to the four setups: ■ Setup 1, ■ Setup 2, ■ Setup 3, ■ Setup 4.

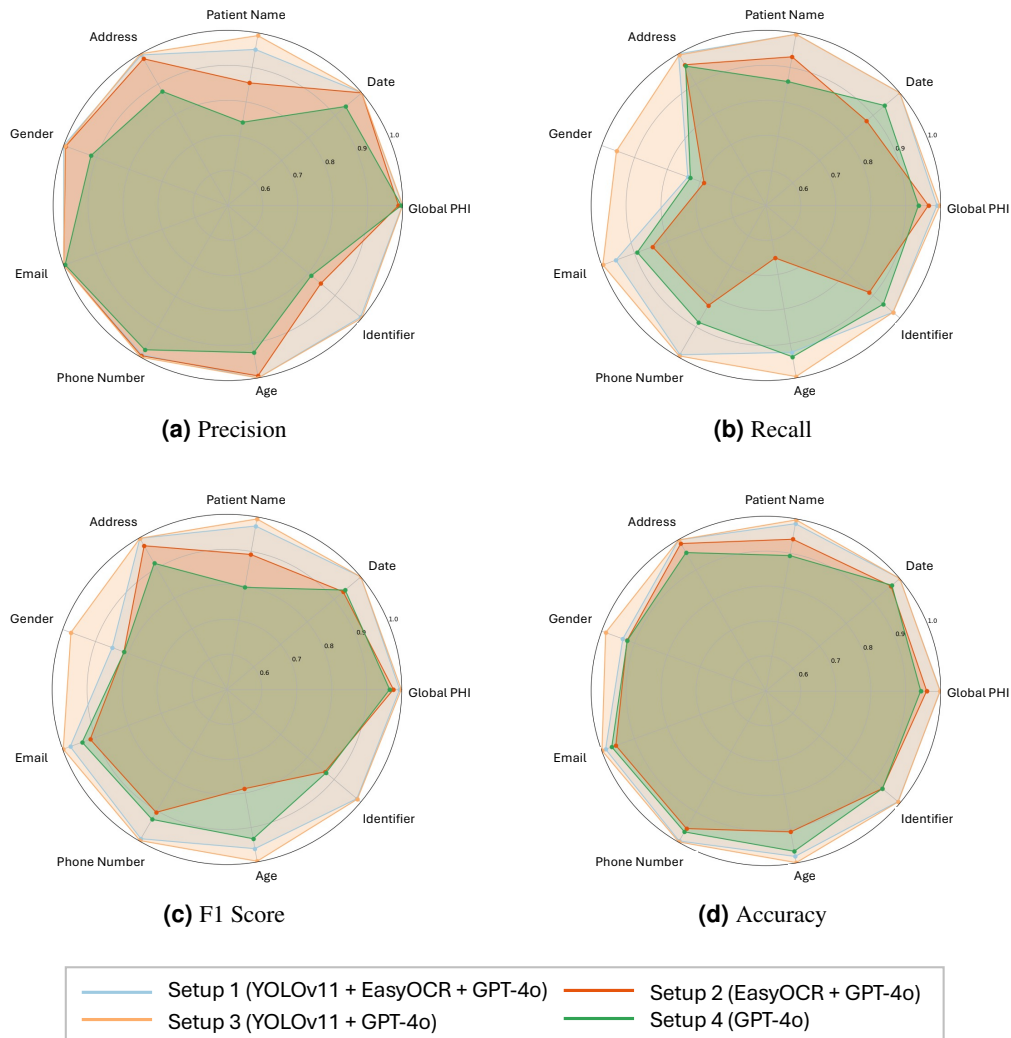


**Figure 6.** The final performance of the PHI detection pipeline evaluated in precision, recall, F1 score, and accuracy.

Setup	Models	Failure rate	Total time	Prompt tokens	Response tokens
1	YOLOv11 + EasyOCR + GPT-4o	4/1000	3736.90 s	1,680,280	226,325
2	EasyOCR + GPT-4o	4/1000	5768.03 s	1,697,703	258,488
3	YOLOv11 + GPT-4o	7/1000	9268.10 s	5,248,046	431,809
4	GPT-4o	91/1000	4197.52 s	3,148,776	251,688

**Table 4.** Comparison of failure rate, total time of analysis, the number of prompt and response tokens for 1,000 test cases. The failure rate is defined as the number of cases that do not successfully complete the entire pipeline. The total time is estimated as the sum of the processing and analysis time required for the entire dataset.



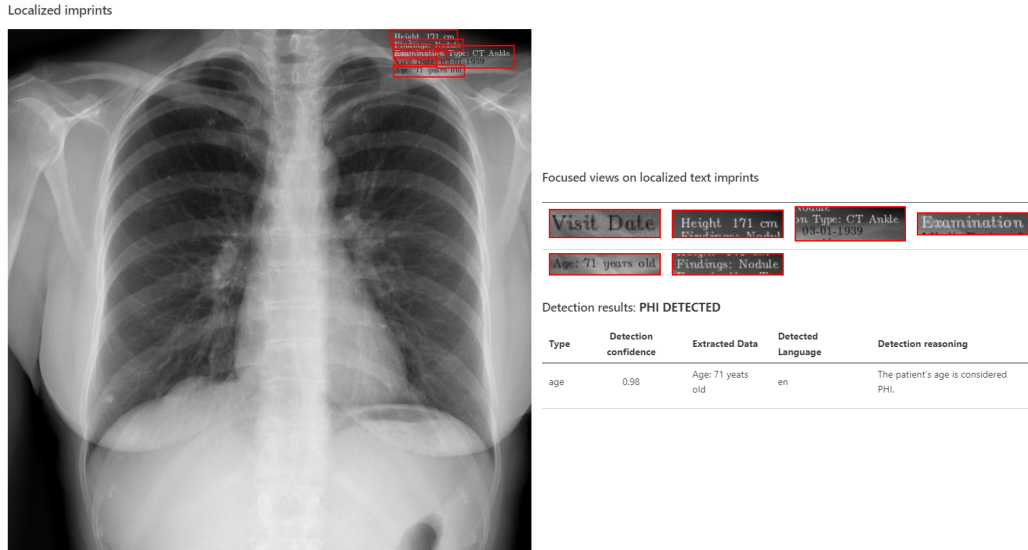


**Figure 7.** When texts appear in blocks, out-of-the-box EasyOCR tries to fit bounding boxes that cover the entire text space. However, the bounding boxes might break the context consistency of the text. For example, `Visit Date` and `03-01-1989` are separated into two different crops, making it harder for the text analyzer to classify PHI content, particularly when a more fine-grain classification of dates is required, e.g., visit date or date of birth.

The results of the four setups presented in [Experiment](#) section are summarized in [Figure 6](#) and [Table 3](#). All four setups demonstrate strong performance in detecting PHI-containing images, with all evaluation metrics (accuracy, precision, recall, and F1 score) exceeding 0.9. Setup 2 (EasyOCR + GPT-4o) and setup 4 (GPT-4o) exhibited slightly lower performance compared to the other setups ([Table 3](#)). However, their performance remains robust, with the overall accuracy at 0.9598 and 0.9428, respectively. Setup 3 (YOLOv11 + GPT-4o) achieves the highest performance, with all four metrics surpassing 0.99. This indicates that the combination of YOLOv11 for text localization and GPT-4o for text analysis excels at identifying images containing PHI. The overall high scores in all evaluation metrics, even in lower-performing setups, suggest that detecting PHI in images is not a particularly challenging task. For instance, despite Setup 2's occasional difficulty detecting more challenging PHI categories, easily detectable PHI items in the same images contribute to scores exceeding 0.95 across all metrics. These findings highlight the feasibility of using the pipeline as a supplementary verification tool for incomplete PHI redaction. For example, research institutions can implement the system to ensure that PHI redaction has been thoroughly applied across all images at the site level before studies begin.

Regarding the classification of PHI categories, date and email are among the top-performing categories. This result is expected because both categories have distinct structures to recognize compared to other classes. On the other hand, gender is the most challenging PHI class to detect, mainly when it appears in abbreviated forms. These single-letter abbreviations often lack accompanying text like `gender`, making detection difficult. If the text extractor fails to recognize the exact character, the text analyzer is left without contextual clues to identify the PHI content and class. This issue is further complicated by potential confusion with single-character markers like `L` or `R`. The bottleneck for fine-grained PHI category classification generally occurs during the text extraction step. When texts are incompletely extracted or when signaling texts are missed, it becomes significantly harder for the text analyzer to classify the content accurately. For example, [Figure 7](#) illustrates how EasyOCR can break text continuity into separate bounding boxes, resulting in missing context and complicating the advanced analysis of PHI terms.

Among the four setups, Setup 2 has the lowest performance. This outcome is expected, as the detection component of EasyOCR is not trained on our simulated data, making it less robust compared to a dedicated YOLOv11 model. Even when EasyOCR is used solely for text extraction (Setup 1), the final pipeline performance lags slightly behind that of GPT-4o (Setup 3). Upon manual examination of specific cases, EasyOCR demonstrates more errors in text extraction compared to using GPT-4o. However, in a majority of cases, GPT-4o, when used as a text analyzer, is powerful enough to infer the intended meaning from improperly extracted text by EasyOCR. This capability results in a comparable performance between Setup 1 and 3. While Setup 3 offers better overall performance, it has a significant drawback: the total analysis time is nearly double that of Setup 1. This is primarily due to the latency associated with querying GPT-4o for extracting text from individual crops.

Consequently, the total number of tokens processed and associated costs are also doubled, as shown in Table 4. Using GPT-4o for the entire pipeline is technically feasible, however it comes with a higher failure rate. Most errors stem from GPT-4o producing unstructured outputs, delivering lower PHI detection performance compared to Setup 1 and 3. While this highlights the impressive vision capability of GPT-4o, it is not yet sufficient to replace dedicated models for text localization and extraction tasks in a single pass.

## Discussion

In this study, we investigate four different setups for pixel-level PHI detection in medical images. For the localization step, we observe the highest performance when using a dedicated object detection model on our simulated data. We recommend using a dedicated object detection model instead of relying on the built-in component of an OCR model (Setup 2) or the localization capability of a multimodal LLM (Setup 4). While EasyOCR might not be an optimal choice for OCR, particularly for text localization, our experimental results demonstrate that separating the localization step and using a model trained explicitly on the target data ensures strong overall performance — even when EasyOCR is used for text extraction (Setup 1). End-to-end GPT-4o (Setup 4) has the drawback that the bounding box coordinates of text regions are not returned, which is essential for subsequent PHI redaction.

For the text extraction step, using an out-of-the-box OCR model such as EasyOCR can achieve a strong final performance. Although GPT-4o can extract text with greater accuracy, the overall improvement in detection rates is minimal due to the compensation effect of the robust text analyzer, as demonstrated in Setups 1 and 3. Therefore, while replacing the conventional OCR model with GPT-4o is feasible, one must weigh the trade-offs of higher latency and associated costs, especially when not using in-house or open-source LLMs, versus the relatively modest gains in the final performance.

GPT-4o is the default and only choice across four setups for the text analyzer. The use of LLMs offers several notable advantages. First, GPT-4o demonstrates strong performance in detecting PHI and classifying it into sub-categories. Secondly, it provides flexibility in adjusting instructions via prompts and configuring output structures, enabling easy adaptation of PHI definition and tasks across studies. However, there are also limitations. GPT-4o outputs may deviate from the configured schema, causing errors that disrupt the pipeline. Additionally, due to the non-deterministic behavior, the model may generate different responses for the same input, which we do not explore deeply in this paper. Future work will investigate and benchmark various prompting strategies and output structuring techniques to enhance the reliability and utility of LLMs in PHI detection pipelines.

## Conclusion

In this paper, we dissect a conventional pixel-level PHI detection pipeline into components and evaluate various setups utilizing an object detection model (YOLOv11), an OCR model (EasyOCR), and an LLM (GPT-4o). Our findings recommend using the LLM for the analysis step, as it offers exceptional, contextual understanding and the flexibility to adjust configurations easily. For the text localization and extraction steps, the optimal approach combines a fine-tuned object detection model with an out-of-the-box OCR tool. This setup outperforms pipelines relying on built-in text detection within OCR models or the vision capabilities of LLMs. Interestingly, we demonstrate that an end-to-end pipeline using only the LLM is feasible. However, the vision capabilities of current LLMs remain limited compared to dedicated vision models. This limitation highlights a space for future exploration to enhance the performance of vision-integrated LLMs in such applications.

## References

1. Center., H. S. C. C. A cost analysis of healthcare sector data breaches (2019).
2. Kline, A., Appadurai, V., Luo, Y. & Shah, S. Medical Image Deidentification, Cleaning and Compression Using Pylogik, DOI: [10.48550/arXiv.2304.12322](https://doi.org/10.48550/arXiv.2304.12322) (2023). ArXiv:2304.12322 [eess].
3. MD.ai. De-Identification - MD.ai Documentation. Available at <https://docs.md.ai/deid/deid/>.
4. Cloud, G. Data de-identification | Cloud Healthcare API | Google Cloud. Available at <https://cloud.google.com/healthcare-api/docs/concepts/de-identification>.
5. Labs, J. S. Data De-identification Tools | NLP Software to De identify PHI under HIPAA. Available at <https://www.johnsnowlabs.com/deidentification/>.
6. Jahan, I., Laskar, M. T. R., Peng, C. & Huang, J. X. A comprehensive evaluation of large Language models on benchmark biomedical text processing tasks. *Comput. Biol. Medicine* **171**, 108189, DOI: [10.1016/j.combiomed.2024.108189](https://doi.org/10.1016/j.combiomed.2024.108189) (2024).

7. Clunie, D. *et al.* Summary of the National Cancer Institute 2023 Virtual Workshop on Medical Image De-identification-Part 1: Report of the MIDI Task Group - Best Practices and Recommendations, Tools for Conventional Approaches to De-identification, International Approaches to De-identification, and Industry Panel on Image De-identification. *J. Imaging Informatics Medicine* DOI: [10.1007/s10278-024-01182-y](https://doi.org/10.1007/s10278-024-01182-y) (2024).
8. Clunie, D. *et al.* Summary of the National Cancer Institute 2023 Virtual Workshop on Medical Image De-identification-Part 2: Pathology Whole Slide Image De-identification, De-facing, the Role of AI in Image De-identification, and the NCI MIDI Datasets and Pipeline. *J. Imaging Informatics Medicine* DOI: [10.1007/s10278-024-01183-x](https://doi.org/10.1007/s10278-024-01183-x) (2024).
9. OpenAI. Hello GPT-4o. Available at: <https://openai.com/index/hello-gpt-4o/>.
10. Wasserthal, J. *et al.* Totalsegmentator: robust segmentation of 104 anatomic structures in ct images. *Radiol. Artif. Intell.* **5** (2023).
11. Huang, Z. *et al.* Bs-80k: The first large open-access dataset of bone scan images. *Comput. Biol. Medicine* **151**, 106221 (2022).
12. Wang, X. *et al.* Chestx-ray8: Hospital-scale chest x-ray database and benchmarks on weakly-supervised classification and localization of common thorax diseases. In *Proceedings of the IEEE conference on computer vision and pattern recognition*, 2097–2106 (2017).
13. Antonelli, M. *et al.* The medical segmentation decathlon. *Nat. communications* **13**, 4128 (2022).
14. Ultralytics. YOLO11 NEW. Available at <https://docs.ultralytics.com/models/yolo11>.
15. Redmon, J., Divvala, S., Girshick, R. & Farhadi, A. You Only Look Once: Unified, Real-Time Object Detection. In *2016 IEEE Conference on Computer Vision and Pattern Recognition (CVPR)*, 779–788, DOI: [10.1109/CVPR.2016.91](https://doi.org/10.1109/CVPR.2016.91) (IEEE, Las Vegas, NV, USA, 2016).
16. EasyOCR. JaidedAI/EasyOCR: Ready-to-use OCR with 80+ supported languages and all popular writing scripts including Latin, Chinese, Arabic, Devanagari, Cyrillic and etc. Available at <https://github.com/JaidedAI/EasyOCR>.
17. Baek, Y., Lee, B., Han, D., Yun, S. & Lee, H. Character Region Awareness for Text Detection, DOI: [10.48550/arXiv.1904.01941](https://doi.org/10.48550/arXiv.1904.01941) (2019). ArXiv:1904.01941 [cs].
18. Baek, J. *et al.* What is wrong with scene text recognition model comparisons? dataset and model analysis. In *International Conference on Computer Vision (ICCV)* (2019).

## Acknowledgements

The authors would like to thank the Bayer team of the AI Innovation Platform for providing computing infrastructure and technical support.

## Appendix

Class	Precision	Recall	F1	Accuracy
Global PHI	0.9988	0.9894	0.9941	0.9990
Date	1.0000	1.0000	1.0000	1.0000
Patient Name	0.9522	0.9962	0.9737	0.9859
Address	0.9960	1.0000	0.9980	0.9990
Gender	1.0000	0.7377	0.8491	0.9357
Email	1.0000	0.9568	0.9770	0.9880
Phone Nr.	0.9922	0.9922	0.9922	0.9960
Age	1.0000	0.9258	0.9615	0.9809
Identifier	0.9957	0.9747	0.9851	0.9930

**Table A1.** PHI detection performance of setup 1 (YOLOv11 + EasyOCR + GPT-4o).

Class	Precision	Recall	F1	Accuracy
Global PHI	0.9879	0.9647	0.9762	0.9598
Date	1.0000	0.8759	0.9339	0.9669
Patient Name	0.8551	0.9308	0.8913	0.9408
Address	0.9835	0.9637	0.9735	0.9869
Gender	0.9941	0.6885	0.8136	0.9227
Email	1.0000	0.8453	0.9162	0.9568
Phone Nr.	0.9954	0.8301	0.9053	0.9548
Age	0.9940	0.6523	0.7877	0.9096
Identifier	0.8468	0.8861	0.8660	0.9347

**Table A2.** PHI detection performance of setup 2 (EasyOCR + GPT-4o).

Class	Precision	Recall	F1	Accuracy
Global PHI	1.0000	0.9976	0.9988	0.9980
Date	1.0000	1.0000	1.0000	1.0000
Patient Name	0.9923	0.9961	0.9942	0.9970
Address	1.0000	0.9959	0.9980	0.9990
Gender	0.9957	0.9549	0.9749	0.9879
Email	1.0000	0.9964	0.9982	0.9990
Phone Nr.	1.0000	0.9961	0.9981	0.9990
Age	1.0000	0.9961	0.9980	0.9990
Identifier	1.0000	0.9747	0.9871	0.9940

**Table A3.** PHI detection performance of setup 3 (YOLOv11 + GPT-4o).

Class	Precision	Recall	F1	Accuracy
Global PHI	0.9959	0.9364	0.9652	0.9428
Date	0.9394	0.9435	0.9414	0.9703
Patient Name	0.7411	0.8591	0.9158	0.9571
Address	0.8760	0.9593	0.9158	0.9571
Gender	0.9167	0.7299	0.8127	0.9219
Email	0.9955	0.8916	0.9407	0.9692
Phone Nr.	0.9757	0.8855	0.9284	0.9659
Age	0.9267	0.9389	0.9328	0.9659
Identifier	0.8114	0.9384	0.8703	0.9351

**Table A4.** PHI detection performance of setup 4 (GPT-4o).